Design Considerations on the Placement of a Wearable UHF-RFID PIFA on a Compact Ground Plane

A. Michel, *Member, IEEE,* R. Colella, *Member, IEEE*, G. A. Casula, *Member, IEEE,* P. Nepa, *Member, IEEE,* L. Catarinucci, *Member, IEEE,* G. Montisci, *Member, IEEE,* G. Mazzarella, *Member, IEEE*, G. Manara, *Fellow, IEEE*

***Abstract*—The robustness of wearable antennas to the human body proximity can be improved by properly placing the radiating element over a ground plane, or by shaping the ground plane, on the basis of the antenna electric and magnetic energy density distributions, aiming to confine the electric energy density in specific regions far from the antenna border. The effectiveness of the above design criterion has been assessed through both numerical analysis and experimental measurements, by optimizing the position of the radiating element of a wearable grounded UHF RFID tag operating at the ETSI band (865-868 MHz), with respect to its ground plane. A flexible tag characterization and performance evaluation platform is used to measure the tag sensitivity as a function of the antenna-body distance.**

***Index Terms*—Wearable antennas, Radio Frequency Identification, body-antenna coupling, tag sensitivity, RFID measurements, antenna energy density, RFID transponders.**

I. Introduction

As largely discussed in the open literature, the human body proximity represents a critical issue for the wearable devices performance [1]-[21]. Since it is a non-homogeneous lossy material, ~~it~~ the human body affects the antenna input impedance and radiation efficiency, leading to a degradation of the overall system performance. Above effect cannot be precisely estimated and considered during the antenna design process, as the dielectric characteristics of the human body depend on the antenna location, and randomly change from person to person. Moreover, the antenna-body distance variation is another important aspect to take into account during the wearable antenna design process. For all these reasons, a wearable antenna is typically designed in proximity of a substrate layer, which approximates the presence of a specific part of the human body. Then, the effect of the antenna-body distance is assessed by either numerical analysis or measurements.

In the recent literature, several papers present an analysis of the performance of wearable antennas as a function of the antenna-body distance. In [3], the input impedance characteristics of an antenna worn on the wrist is investigated, under the dry/wet skin conditions, demonstrating that the skin moisture condition and the differences among individuals have a great effect on the input impedance in the lower frequency range (1-100 MHz). In [4]-[5], Kellomaki *et al*. investigated the effect of the human body on a small wearable single-layer dipole tag antenna for Ultra High Frequency (UHF) Radio Frequency Identification (RFID) applications. In this case, measured results in terms of realized gain and mismatch factor demonstrate that the body surface may introduce a significant antenna performance degradation. In [6], the analysis is repeated for a single-layer wearable antenna for GPS applications at 1575MHz. In [7], a parametric study is described by considering six single-layer antennas operating at 2.4-2.48 GHz. The effects of both antenna location and antenna-body distance are measured in terms of input impedance mismatching, radiation patterns, gain and efficiency. Also Casula *et. al* investigated the effect of the human body on single layer antennas [8], [9].

In general, even though single-layer antennas may be used for wearable applications, it is well-formed opinion that a relatively large ground plane is beneficial to limit the effect of the human body proximity on the antenna performance [6]-[16]. However, at low frequency bands (e.g. f<500MHz), there is no room to implement a large ground plane able to decouple the antenna from the body, nor does the wearer's body act as an effective reflector to reduce back radiation and increase antenna gain [1]. It is worth noting that, regardless the operation frequency or application, a wearable antenna must be as comfortable and unobtrusive as possible, and, as a consequence, it should be physically small. Then, it follows that low-frequency wearable antennas are electrically small, and only one of the two energy densities dominates in the antenna near-field (NF) region. Since the human body is a non-magnetic material, electrically small magnetic antennas perform better than electrically small electric antennas, when they operate close to, or inside, the human body [20]-[21]. On the other hand, several body-centric wireless systems operate at relatively high frequency, such as those based on technologies like UHF RFID, Wireless Local Area Network (WLAN) or Bluetooth. For these applications, the antenna physical size is comparable with the wavelength at the operating frequency, and it is much smaller than the human body size. For example, wearable patch antennas at 923 MHz [10] and 2.4 GHz [11], [12] have been considered. As a general guideline, in [10] authors assert that, for a high and stable radiation efficiency, the ground plane should have a length of at least 1.5 times the largest length of the antenna patch. In [11], a Planar Inverted-F Antenna (PIFA) is suggested, even though it may experience more fabrication issues than a patch antenna, due to the presence of the shorting pin. Moreover, in [13] the effect of the ground plane shape of a wearable monopole antenna has been evaluated in terms of resonant frequency, input impedance and radiation patterns, at 1.8 GHz and 2.45 GHz. Finally, in [14], [15] a 14×100 mm^2 planar antenna with a full ground plane is described, showing a high robustness with respect to the human body.

A proper ground plane shaping and sizing may help to make the antenna less obtrusive and easy to be worn. In [16], PIFA antennas have been numerically analyzed at different operating frequencies (from 868 MHz to 2.4 GHz), showing that the antenna performance is correlated

to the distribution of the electric and magnetic energy densities in the antenna near-field region close to the ground plane border; a criterion is derived for choosing a proper shape of the antenna ground plane to improve the antenna robustness with respect to the body–antenna coupling, with a minimal impact on the antenna size. In particular, the antenna robustness has been assessed by means of two metrics, namely the power transmission coefficient (τ) and the radiation efficiency (η), which have been numerically evaluated versus the body-antenna distance. In [8], the analysis has been extended to ungrounded antennas, and a preliminary experimental validation has been carried out by measuring the input impedance variation as a function of the distance between the antenna and a human body phantom. Such a measurement confirmed that the power transmission coefficient (τ) variation can be minimized by extending the antenna layout toward the directions close to an electric energy density peak.

In this paper, the effect of the position of the radiating element of a wearable antenna with respect to its ground plane is investigated. Differently from other papers in the scientific literature, a physical insight on the optimal placement of the radiating element on its compact ground plane is given, by exploiting the energy-based design criterion presented in [16]. This may allow an antenna designer for properly shaping the ground plane, so improving the wearable antenna robustness to the human body presence, while limiting the antenna size. In particular, starting from [22], a UHF RFID tag based on an ad-hoc PIFA has been designed and fabricated. Without loss of generality, UHF RFID technology has been considered, but similar considerations may be applied to antennas for different microwave applications. An exhaustive simulated analysis has been carried out to evaluate the effect of the radiating element position with respect to the ground plane on the tag antenna power transmission coefficient (τ) and radiation efficiency (η), when the antenna-body distance varies.

In general, in a wireless communication system, the variations of both the input impedance, and then τ, and the radiation efficiency (η) are responsible for the overall system performance degradation. More in detail, the antenna gain (G) is usually considered in a link budget, which is proportional to the radiation efficiency of a specific radiating element. From a practical point of view, the antenna gain is easier to be measured than the radiation efficiency. Therefore, an experimental validation of the behavior of the product $\tau \times G$, which is proportional to $\tau \times \eta$, has been performed in this paper, so as to fully assess the effectiveness of the energy-based design criteria presented in [16]. To do so, the tag performance evaluation platform in [23] has been used to measure the main metrics characterizing a wearable RFID tag (*i.e.* the power transfer coefficient and the antenna radiation efficiency) as a function of the distance between the tag and a human-body phantom. The tag sensitivity has been computed through a suitable post-processing of the measured backscattered signal, and an estimate of the $\tau \times G$ product has been lastly obtained.

Simulated and measured results obtained for three antenna layouts have been compared, confirming the effectiveness of the design criteria proposed in [16]. Remarkably, the energy-based criterion has been considered in some recent papers for antennas other than PIFAs [17]-[19]. In particular, in [19], the authors designed a wearable textile antenna inspired by a folded cavity. In presence of dielectric loading, frequency and bandwidth variations have been experienced, and the energy-based criterion has been adopted to increase the isolation between the antenna and the human body.

The rest of the paper is organized as follows: in Section II, the antenna layout and parametric simulated results obtained by using CST Microwave Studio® are analyzed. In Section III, after describing the measurement setup, the experimental results are shown and discussed. Then, final conclusions and remarks are given in Sect. IV.

II. Antenna Layout and Numerical Analysis

The ad-hoc PIFA, whose design starts from [22], has been fabricated on two 1.57-mm-thick RT/duroid 5870 substrates (ε_r=2.3, tanδ=0.002) in a stacked configuration, so obtaining an antenna thickness H=3.2 mm. The antenna layout is shown in Fig. 1a, and its geometrical dimensions are listed in Table 1. The overall antenna size is 53mm×53mm, which corresponds to 0.154λ×0.154λ, being λ the free-space wavelength at 866.5MHz. The antenna consists of a patch element on which a two-arm slot has been etched; the patch is short-circuited through 11 copper rivets. In the simulation model, the input port is placed between the slot arms, so as to model the feeding point corresponding to the microchip of the RFID tag. The size of the two slot arms is effective in controlling both the real and imaginary parts of the antenna input impedance, so allowing to obtain a satisfactory impedance matching with different commercial chips. In this paper, the slot has been designed to achieve a τ higher than 0.8 with a Monza 3 chip (Z_{CHIP}=13-j151 Ω) [24].

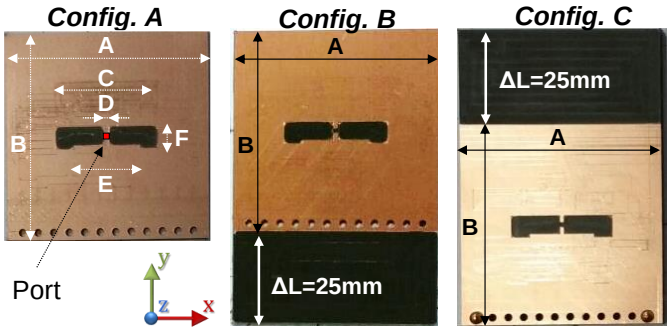

(a) (b) (c)

Fig. 1. (a) Prototype of the designed wearable UHF-RFID PIFA. In (b) and (c), the two modified versions with enlarged ground plane are shown, where the PIFA open side is (b) close to or (c) far from the ground plane edge.

TABLE 1
ANTENNA GEOMETRICAL PARAMETERS

Parameter	Value	Parameter	Value
A	53 mm	**E**	17 mm
B	53 mm	**F**	6 mm
C	27 mm	**D**	1 mm

In order to improve the antenna robustness with respect to the human body coupling, the ground plane size must be suitably increased to optimize the antenna performance, without enlarging too much the overall antenna size. The approach discussed in [8], [16] suggests a ground plane extension toward the region where the electric energy density exhibits a peak. Fig. 2 shows the simulated electric energy density distribution, inside and around the dielectric substrate of the antenna configuration in Fig. 1a.

According to [16], three antenna versions have been considered (Fig. 1):

- ***Config. A*** (Fig. 1a) represents the original antenna, whose dimensions are listed in TABLE 1;
- ***Config. B*** (Fig. 1b) is obtained from ***Config. A*** by increasing the ground plane size and placing the PIFA open side **close** to the ground plane edge;
- ***Config. C*** (Fig. 1c) is obtained from ***Config. A*** by increasing the ground plane size and placing the PIFA open side **far** from the ground plane edge.

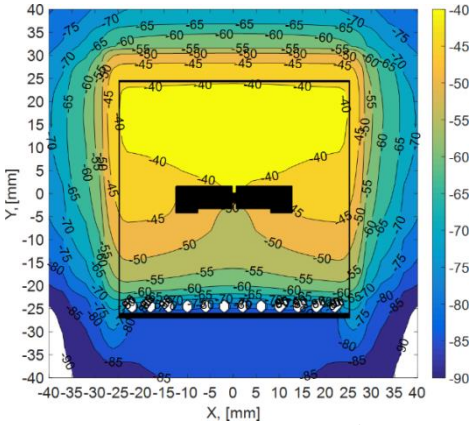

Fig. 2. Electric energy density distribution (dBJm^{-3}) on a XY plane inside the wearable PIFA of Fig. 1a.

It should be noted that the slot dimension is the same for the three prototypes, and it has been optimized to maximize the input impedance matching with a Monza 3 chip [24]. As discussed in [16], [8], η and τ can be considered to study the antenna robustness with respect to the distance (d) between the antenna and the human body. The power transmission coefficient is calculated as

$$\tau(d) = 1 - \left| \frac{Z_{IN}(d) - Z_0^*}{Z_{IN}(d) + Z_0} \right|^2 = \frac{4\,\mathrm{Re}(Z_0)\,\mathrm{Re}(Z_{IN}(d))}{\left| Z_0 + Z_{IN}(d) \right|^2} \qquad (1)$$

wherein Z_{IN} is the antenna input impedance, and Z_0 is a reference impedance (*i.e.* $Z_0 = Z_{CHIP} = 13 - j151\,\Omega$ for the Monza 3 chip). In order to numerically analyze the interaction between the antenna and the human body, an equivalent model at 866.5 MHz, consisting in a 5-cm-thick material with $\varepsilon_r = 2/3$, $\varepsilon_{r\_muscle} = 36$, and $\sigma = 2/3\ \sigma_{muscle} = 0.62$ S/m, has been added to the simulation scenario [8]. Thus, the wearable antenna performance robustness has been estimated by means of two metrics, τ and $\tau \times \eta$, which are computed as a function of both d and frequency, in a range close to the ETSI UHF RFID operative band (865-868 MHz). In addition, the effect of the antenna radiating element position with respect to its ground plane has also been evaluated. In particular, a rectangular ground plane which fits an overall available area of 53×78mm^2 has been considered. The radiating element of 53×53mm^2 has been placed in various positions with respect to the ground plane, and, for each position, the τ and $\tau \times \eta$ variations have been computed. Hence, it is possible to choose the optimal antenna positioning, i.e., the configuration that allows for the best antenna robustness with respect to the body coupling effect.

As shown in Fig. 3, the distance Δ between the PIFA open side and the ground plane border has been increased from Δ=0mm (***Config. B***) to Δ=25mm (***Config. C***). In Fig. 4 and Fig. 5, the simulated τ and $\tau \times \eta$ variations, as a function of the distance (x-label) and frequency (y-label), are shown for six specific cases, corresponding to Δ=0mm (***Config. B***), Δ=5mm, Δ=10mm , Δ=15mm, Δ=20mm and Δ=25mm (***Config. C***).

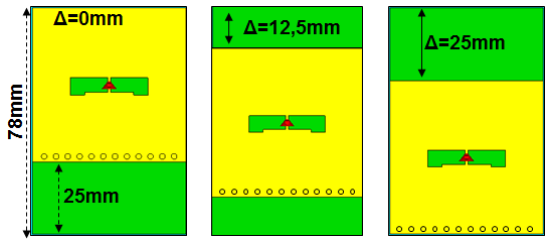

(a) (b) (c)

Fig. 3. Simulated layouts for three different ground plane extensions (Δ): (a) Δ=0mm (**Config B**), (b) Δ=12.5mm and (c) Δ=25mm (**Config C**).

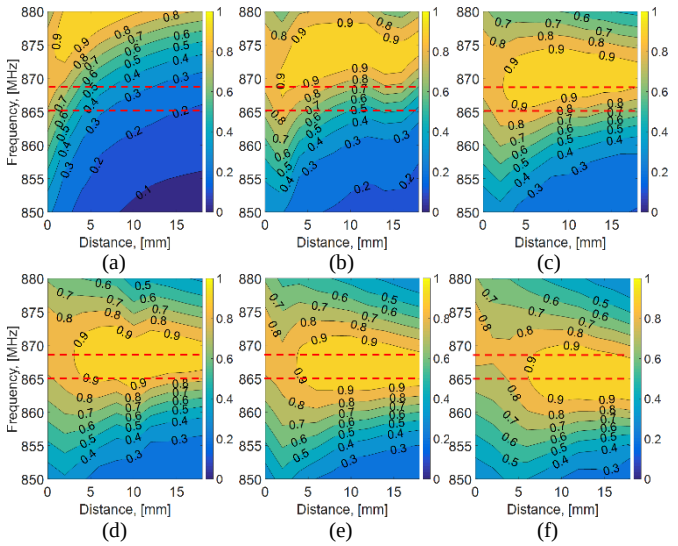

Fig. 4. Simulated results for τ vs. frequency (*y*-label) and antenna-body distance (*x*-label), for different values of Δ: (a) Δ=0mm (***Config. B***), (b) Δ=5mm, (c) Δ=10mm, (d) Δ=15mm, (e) Δ=20mm, (f) Δ=25mm (***Config. C***). Dashed lines indicate the lower and upper frequency limits of the ETSI UHF-RFID band.

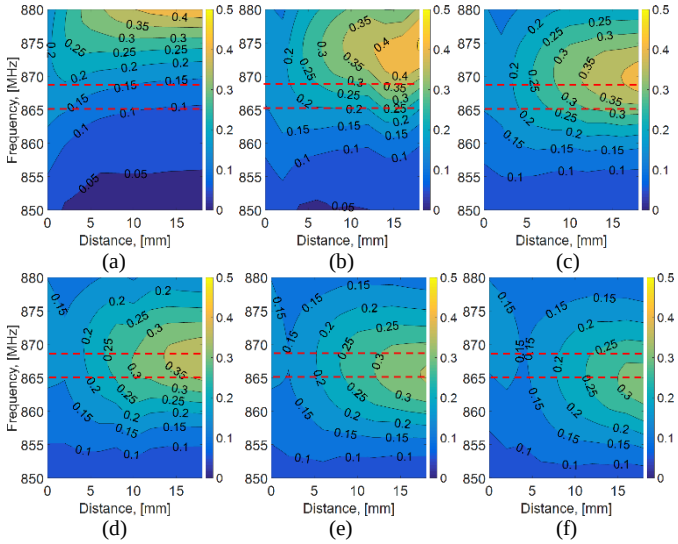

Fig. 5. Simulated results for τ×η vs. frequency (*y*-label) and antenna-body distance (*x*-label), for different values of Δ: (a) Δ=0mm (***Config. B***), (b) Δ=5mm, (c) Δ=10mm, (d) Δ=15mm, (e) Δ=20mm, (f) Δ=25mm (***Config. C***). Dashed lines indicate the lower and upper frequency limits of the ETSI UHF-RFID band.

It is apparent that the robustness of the antenna with respect to the presence of the human body can be significantly increased by extending both the metal plate and the dielectric substrate toward the antenna section corresponding to the location of the maximum of the electric energy density (***Config. C***). When the antenna is attached to the human body phantom (d=0mm), the power transmission coefficient in the 865-868 MHz band is comparable for all six antenna configurations (Fig. 4). However, when fixing the operative frequency and increasing the distance *d*, ***Config. C*** (Fig. 4f) experiences a smaller variation of τ with respect to the other configurations. Nevertheless, from results in Fig. 4 it appears that the higher is the value of Δ, the more stable is the value of τ in the entire operative frequency band. Similar considerations apply to $\tau \times \eta$ (Fig. 5). This is a desirable feature, especially for applications with higher percentage bandwidth. The results shown in Figs. 4 and 5 confirm that a larger value of Δ is effective in avoiding a frequency shift, as well as in providing a more robust antenna configuration. In other terms, for a given available area on the ground plane (*e.g.* 78×25 mm^2 in Fig. 3), the position of the radiating element should be chosen in order to maximize the distance between the ground plane border and the energy electric density peak. For the presented example, the maximum value of τ at the central frequency of 866 MHz is achieved for Δ>15mm, while a significant performance degradation can be observed if Δ decreases from 15 mm to 0. These considerations are not limited to the discussed PIFA antenna, but can be extended to a large class of antennas for body-centric communications, with the sole limitation that they must exhibit a small variation of the energy density distributions within their operative frequency band ([8], [9], [16]-[19]).

In Fig. 6, the τ (Fig. 6a) and $\tau \times \eta$ (Fig. 6b) curves have been plotted as a function of the antenna-body distance, for the three antenna layouts shown in Fig. 1, and for three frequencies of the ETSI UHF-RFUD band: 865 MHz, 866.5 MHz and 868 MHz.

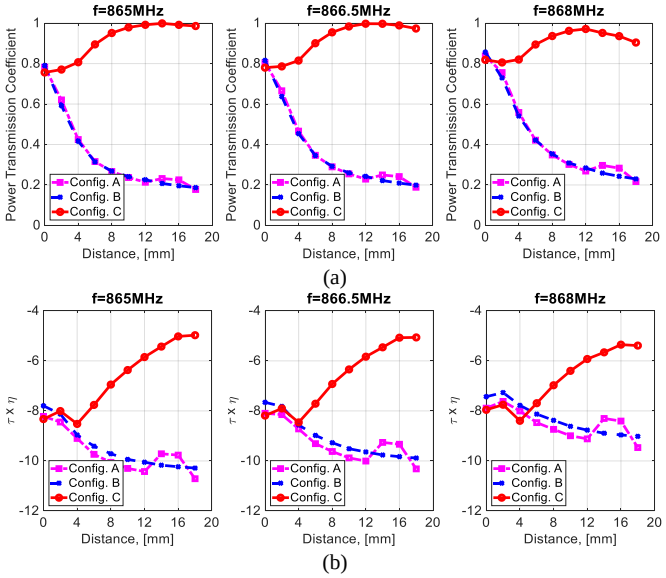

Fig. 6. Simulated results for (a) τ and (b) $\tau \times \eta$ vs. the antenna-body distance, for the three configurations shown in Fig. 1 and for the lower (f=865MHz), central (f=866.5MHz) and higher (f=868MHz) frequencies of the operative ETSI UHF RFID band.

It should be noted that the ***Config. C*** performance is generally better and more stable than the ***Config. A*** and ***Config. B***, both in terms of τ and $\tau \times \eta$. In particular, when the antenna-body distance varies from 0 to 18mm, the parameter τ of ***Config. C*** assumes values higher than 0.8, while its $\tau \times \eta$ is always higher than -8 dB. This is valid in the whole ETSI band (865-868 MHz). On the other hand, ***Config. A*** and ***Config. B*** have similar performance when varying the antenna-body distance, but their behavior is significantly worse than ***Config. C***. This is also confirmed by the results shown in Fig. 7, where the simulated ***Config. A*** performance in terms of τ and $\tau \times \eta$ is plotted as a function of the frequency (y-label) and the antenna-body distance (x-label). Such distributions are similar to those related to ***Config. B*** (Fig. 4a and Fig. 5a), which has a larger ground plane. Therefore, increasing the ground plane size towards the direction of the PIFA short-circuit side, not only makes the antenna more obtrusive and uncomfortable to the wearer, but is also useless from the performance improvement point of view.

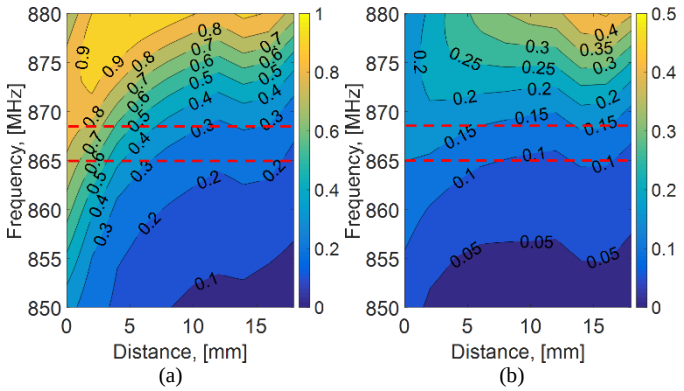

Fig. 7. Numerical performance of ***Config. A*** in terms of (a) τ and (b) $\tau \times \eta$ vs. the frequency (y-label) and the antenna-body distance (x-label). It should be noted that these distributions are comparable with those obtained with ***Config. B***, which means that the ground plane extension is useless. Dashed lines indicate the lower and upper frequency limits of the ETSI UHF-RFID band.

III. Experimental Validation

An experimental validation has been carried out to assess the numerical analysis presented in Section II. A preliminary validation has been presented in [16], where the antenna input impedance has been measured by means of a Vector Network Analyzer for different antenna-body distances. The simulation and measurement results presented in [16] are in good agreement, demonstrating that a layout extension toward the antenna border where the electric energy density exhibits a maximum may improve the antenna robustness to the human body proximity, at least in terms of τ.

To extend such an experimental analysis, and also evaluate the behavior of $\tau \times \eta$ as a function of the antenna-body distance, the flexible tag characterization and performance evaluation platform proposed and validated in [23] has been used. The system is mainly composed of a special multi-programmable UHF RFID reader board, ThingMagic Mercury 6e (M6e), having its RF interface connected to a circularly polarized patch antenna with gain equal to 5.1 dBi. The reader board allows to modify both the emitted power (in the range 5 – 31.5 dBm, in steps of 0.5 dB) and the working frequency in the whole RFID bandwidth. It is worth highlighting that the wide power excursion along with the good power resolution of this reader are suitable features to allow for the implementation of a measurement procedure based on the iterative research of the tag activation power threshold $P_{tx,ON}$. The general purpose setup presented in [23] has been properly customized so to guarantee accurate measurements in the specific use case. In particular, an artificial model of the human tissue has been synthesized in the laboratory by

means of a specific saline solution, to mimic the body average dielectric properties [8]. The saline solution has been inserted in a PVC tank having a thickness of 1.5 mm (whose dielectric parameters have been properly taken into account), arranged in front of the reader board antenna, and placed in anechoic environment, as shown in Fig. 8.

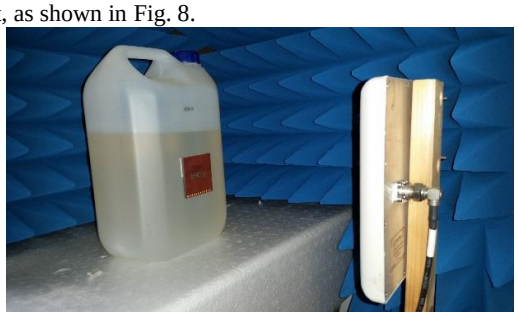

Fig. 8. The tag under test applied on the saline solution tank emulating the human tissue, inside the anechoic environment.

In order to estimate the behavior of the term $\tau \times \eta$ when varying d, an enhancement of the theoretical model proposed in [23] for the over-the-air evaluation of the whole tag sensitivity S_{tag} has been carried out by deriving the following formula of $\tau \times G_{tag}$:

$$\tau \times G_{tag} = \frac{S_{chip} \cdot \left(4\pi d_{tag}\right)^2}{P_{tx,\mathrm{ON}} \cdot G_{tx} \cdot \lambda^2 \eta_{plf} \cdot A_{cable}}, \qquad (1)$$

where the term $P_{tx,ON}$ denotes the minimum power value emitted by the RFID reader which turns on the chip (in correspondence of the chip sensitivity S_{chip}), G_{tx} is the maximum gain of the reader antenna, λ is the wavelength in free space, d_{tag} is the distance between RFID tag and reader; η_{plf} is the polarization loss factor depending on the tag antenna structure; A_{cable} is the cable attenuation. Once implemented (1) in the measurement setup, the term $\tau \times G_{tag}$ can be straightforwardly evaluated for the three considered antennas when the distance d between tag and human tissue is varying. It is worth underlining that the simulated radiation patterns (Fig. 9) are substantially the same for each configuration, since the overall antenna size does not change. Specifically, in Fig. 9 the radiation patterns of the three configurations are shown for two antenna-body distances: d=0 (antenna is attached to the human body) and d=18mm. Differently from the ϕ=0° cut, the radiation patterns on the ϕ=90° plane are asymmetrical due to the asymmetry of the antenna layout (Fig. 1). Also, the maximum directivity direction is almost the same for all the configurations and for the two considered antenna-body distances, and coincides with the direction orthogonal to the antenna surface. In fact, the antenna electrical size of the three prototypes is similar, so the antenna effective areas are comparable, as for the antenna directivities. This allows for a fair comparison among the antenna layouts, focusing to the body proximity effect on the antenna performance. Consequently, the estimated $\tau \times G_{tag}$ value is directly proportional to the $\tau \times \eta$ product numerically evaluated.

In Fig. 10a, the measured tag sensitivity is shown as a function of the antenna-body distance. Thus, by assuming a chip sensitivity equal to -20dBm [24], the $\tau \times G_{tag}$ product has been estimated and plotted in Fig. 10b, as a function of the tag-reader antenna distance, d, in the range between 0 (tag attached to the human body) and 18 mm

Driven by the Received Signal Strength Indicator (RSSI) provided by the RFID reader used in the experimental setup, for each measurement point a fine adjustment of the alignment between reader antenna and tag has been carried out so to guarantee the maximum power transfer in each test. Since the far field patterns are very similar for the three configurations A, B, and C, only slight variations have been necessary during the measured data collection.

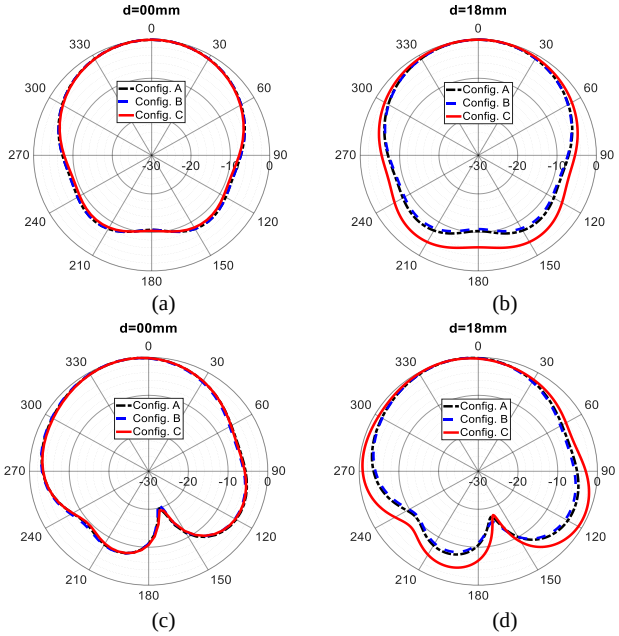

Fig. 9. Simulated radiation pattern for the three configurations at two antenna-body distances, d, and at two cut planes: ϕ=0° at (a) d=0mm and (b) d=18mm; ϕ=90° at (c) d=0mm and (d) d=18mm.

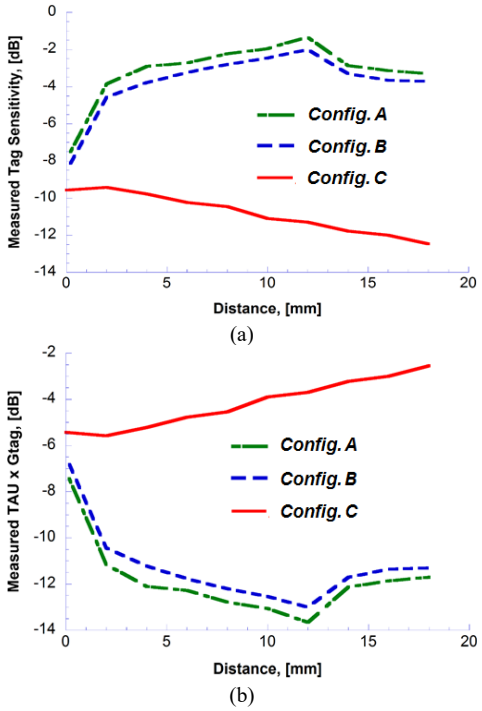

Fig. 10. (a) Measured tag sensitivity of the three UHF RFID tag configurations, as a function of the antenna-body phantom distance (at f=865 MHz): (b) $\tau \times G_{tag}$, which has been computed for a Monza 4 chip with a sensitivity equal to -20dBm.

Four 5x5-mm^2 bi-adhesive pads of low density polyethylene foam (dielectric constant close to 1) placed at the four corners of the tag have been used for supporting and spacing the tag during the test. When attached to the human body phantom, the tag sensitivities of the proposed tags are similar. However, when increasing the antenna-body distance, the ***Config. C*** tag sensitivity experiences a small variation, differently from both ***Config. A*** and ***Config. B,*** whose tag sensitivity exhibits a 4dB increase with a distance variation as small as 2mm. Therefore, ***Config. C*** is significantly more robust to the presence of the human body. Moreover, even though the two antenna radiating elements and ground planes have the same size, the measured tag sensitivity of ***Config. C*** is significantly lower than the ***Config. B***'s one. This improvement has been obtained by simply shifting the radiating element with respect to the 78×25 mm^2 rectangular ground plane. Similarly, the estimated $\tau \times G_{tag}$ product measured for the ***Config. C*** tag is higher than the ***Config. B***'s one, and more stable when increasing the antenna-body distance. Finally, a particular behavior is experienced in ***Config. A*** and ***Config. B*** cases, where a maximum is found for both the sensitivity and $\tau \times G_{tag}$ when d is close 12mm. Assuming G_{tag} quite stable in the direction of maximum radiation, this behavior is reasonably due to the antenna impedance variation caused by the background material which, of course, impacts upon τ and consequently upon both parameters here analyzed.

It can be summarized that ***Config. C*** is the one guaranteeing the better performance, thanks to the ground plane extended toward the direction where a peak of electric density is located. This result might be deduced also by considering the PIFA radiation mode. Indeed, the PIFA antenna mainly radiates from its open side, so that by intentionally increasing the shielding with the background in such a region, higher robustness to the body-coupling can be achieved. Nevertheless, the result is much more general and can be applied to a variety of antennas characterized by a more complex radiating element.

IV. Conclusion

The proper positioning of the radiating element of a Planar Inverted-F antenna with respect to its ground plane borders has been used as an approach to improve the robustness of a wearable antenna with respect to the human body proximity. The results confirmed that antenna robustness is improved when the electric energy peaks appearing in the antenna reactive near-field region are far from the borders of the ground plane. The analysis has been carried out both numerically and experimentally, by means of a performance evaluation platform developed for RFID tags operating at the ETSI UHF RFID band (865-868 MHz). Nonetheless, the above criteria can be extended to a large class of antennas for body-centric communications, whenever they exhibit a small variation of the energy density distributions within their operative frequency band.

References

[1] P. Nepa and H. Rogier, "Wearable antennas for off-body radio links at VHF and UHF bands (below 1 GHz): challenges, state-of-the-art and future trends," *IEEE Ant. Propag. Magaz*., vol. 57, no. 5, pp. 30-52, Oct 2015.

[2] A. Michel, K. Karathanasis, P. Nepa and J.L. Volakis, "Accuracy of a Multi-probe Conformal Sensor in Estimating the Dielectric Constant in Deep Biological Tissues", *IEEE Sensors Journal*, vol. 15, no. 9, pp. 5217-5221, Sept. 2015.

[3] D. Muramatsu, F. Koshiji, K. Koshiji and K. Sasaki, "Input impedance analysis of wearable antenna and its experimental study with real human body," *2014 IEEE International Conference on Consumer Electronics (ICCE)*, Las Vegas, NV, 2014, pp. 151-152.

[4] T. Kellomäki, T. Björninen, L. Ukkonen and L. Sydänheimo, "Shirt collar tag for wearable UHF RFID systems," *Proceedings of the Fourth European Conference on Antennas and Propagation*, Barcelona, Spain, 2010, pp. 1-5.

[5] T. Kellomaki, "On-Body Performance of a Wearable Single-Layer RFID Tag," *IEEE Antennas and Wireless Propagation Letters*, vol. 11, pp. 73-76, 2012.

[6] T. Kellomaki, J. Heikkinen and M. Kivikoski, "One-Layer GPS Antennas Perform Well near a Human Body," *European Conference on Antennas and Propagation, EuCAP 2007*, Edinburgh, pp. 1-6, 2007.

[7] A. Alomainy, Y. Hao and D. M. Davenport, "Parametric Study of Wearable Antennas with Varying Distances from the Body and Different On-Body Positions," *2007 IET Seminar on Antennas and Propagation for Body-Centric Wireless Communications*, London, 2007, pp. 84-89.

[8] G. A. Casula, A. Michel, G. Montisci, P. Nepa and G. Valente, "Energy-Based Considerations for Ungrounded Wearable UHF Antenna Design," *IEEE Sensors Journal*, vol. 17, no. 3, pp. 687-694, Feb. 2017.

[9] G. A. Casula, G. Montisci, A. Michel, P. Nepa, "Robustness of complementary wearable ungrounded antennas with respect to the human body," *Journal of Electromagnetic Waves and Applications*, Vol. 31, Issue 16, pp. 1685-1697, November 2017.

[10] C. Hertleer, H. Rogier, L. Vallozzi and L. Van Langenhove, "A Textile Antenna for Off-Body Communication Integrated Into Protective Clothing for Firefighters," *IEEE Transactions on Antennas and Propagation*, vol. 57, no. 4, pp. 919-925, April 2009.

[11] E. S. Florence, M. Kanagasabai, and G. N. M. Alsath, "An investigation of a wearable antenna using human body modelling", *Applied Computational Electromagnetics Society Journal*, Vol. 29 Issue 10, pp. 777-783, Oct. 2014.

[12] H. Giddens, D. L. Paul, G. S. Hilton and J. P. McGeehan, "Influence of body proximity on the efficiency of a wearable textile patch antenna," 2012 European Conference on Antennas and Propagation (EUCAP), Prague, pp. 1353-1357, 2012.

[13] M. Shafi, M. I. Khattak, N. Khan and M. Saleem, "Ground plane shape effects on around the body area network at 1.8GHz and 2.45GHz," 2014 IEEE Region 10 Symposium, Kuala Lumpur, 2014, pp. 426-429.

[14] S. M. Abbas, K. P. Esselle, L. Matekovits, M. Rizwan and L. Ukkonen, "On-body antennas: Design considerations and challenges," 2016 URSI International Symposium on Electromagnetic Theory (EMTS), Espoo, pp. 109-110, 2016.

[15] S. M. Abbas, Y. Ranga and K. P. Esselle, "Sensitivity of a wearable printed antenna with a full ground plane in close proximity to human arm," 2015 9th European Conference on Antennas and Propagation (EuCAP), Lisbon, pp. 1-4, 2015.

[16] G.A. Casula, A. Michel, P. Nepa and G. Montisci, "Robustness of Wearable UHF-Band PIFAs to Human-Body Proximity", *IEEE Trans. Antennas Propag.*, vol. 64, no. 5, pp. 2050-2055, May 2016.

[17] G. Li, Y. Huang, G. Gao, X. Wei, Z. Tian and L. A. Bian, "A Handbag Zipper Antenna for the Applications of Body-Centric Wireless Communications and Internet of Things," *IEEE Transactions on Antennas and Propagation*, vol. 65, no. 10, pp. 5137-5146, Oct. 2017.

[18] G. Li, Z. Tian, G. Gao, L. Zhang, M. Fu and Y. Chen, "A Shoelace Antenna for the Application of Collision Avoidance for the Blind Person," *IEEE Transactions on Antennas and Propagation*, vol. 65, no. 9, pp. 4941-4946, Sept. 2017.

[19] S. P. Pinapati, D. C. Ranasinghe and C. Fumeaux, "Textile Multilayer Cavity Slot Monopole For UHF Applications," *IEEE Antennas and Wireless Propagation Letters*, vol. 16, pp. 2542-2545, 2017.

[20] M. Manteghi and A.A.Y. Ibraheem, "On the study of the Near-Fields of Electric and Magnetic Small Antennas in Lossy Media," *IEEE Transactions on Antennas and Propagation* , vol. 62, no. 12, pp. 6491-6495, Dec. 2014.

[21] R. M. Makinen, T. Kellomaki, "Body effects on thin single-layer slot, self-complementary, and wire antennas," *IEEE Transactions on Antennas and Propagation*, vol. 82, no. 1, pp. 385-392, Jan. 2014.

[22] C. Occhiuzzi, S. Cippitelli, and G. Marrocco, "Modeling, design and experimentation of wearable RFID sensor tag", *IEEE Transactions on Antennas and Propagation* , 58(8), pp. 2490–2498, 2010.

[23] R. Colella, L. Catarinucci, P. Coppola, and L. Tarricone, "Measurement Platform for Electromagnetic Characterization and Performance Evaluation of UHF RFID Tags," *IEEE Trans. on Instrumentation and Measurement*, vol. 65, no. 4, pp. 905-914, Apr 2016.

[24] Impinj Monza 3 RFID chip Datasheet [Online]. Available: https://www.impinj.com